Metabolic limits on classical information processing by biological cells

Chris Fields[1] and Michael Levin[2]

[1] *23 Rue des Lavandières*
11160 Caunes Minervois, FRANCE
fieldsres@gmail.com
ORCID: 0000-0002-4812-0744

[2] *Allen Discovery Center at Tufts University*
Medford, MA 02155 USA
michael.levin@tufts.edu
ORCID: 0000-0001-7292-8084

August 16, 2021

Abstract

Biological information processing is generally assumed to be classical. Measured cellular energy budgets of both prokaryotes and eukaryotes, however, fall orders of magnitude short of the power required to maintain classical states of protein conformation and localization at the Å, fs scales predicted by single-molecule decoherence calculations and assumed by classical molecular dynamics models. We suggest that decoherence is limited to the immediate surroundings of the cell membrane and of intercompartmental boundaries within the cell, and that bulk cellular biochemistry implements quantum information processing. Detection of Bell-inequality violations in responses to perturbation of recently-separated sister cells would provide a sensitive test of this prediction. If it is correct, modeling both intra- and intercellular communication requires quantum theory.

Keywords: Bioenergetics; Decoherence; Metabolism; Molecular dynamics; Protein conformation; Protein localization

1 Introduction

Whether biological cells employ quantum coherence for information processing has been controversial since Schrödinger [1] introduced the idea. The question gained prominence when Hameroff and Penrose [2] proposed that neuronal microtubules function as quantum computers and Tegmark [3] countered that decoherence renders quantum computation in such systems infeasible; see [4, 5, 6] for continuing discussion. Recent studies in quantum biology have largely focused on the role of single-protein scale coherence in photoreception and magnetoreception in a variety of systems (see [7, 8, 9] for reviews). Both experimental reproducibility and theoretical interpretation remain significant sources of controversy [10, 11].

Here we consider this question of biomolecular coherence from a bioenergetic perspective. While some still contest it [12, 13], since the pioneering efforts of Turing [14], Polanyi [15], Liberman [16], and Rosen [17] among others, the idea that biomolecular processes are at bottom informational processes has become commonplace. Indeed any sequence of state changes can, in principle, be considered "information processing" [18] and assigned a thermodynamic cost independently of any higher-level functional considerations. State changes can be either logically reversible or logically irreversible. A process $\psi_i \rightarrow \psi_j$ is logically reversible if ψ_i can be fully recovered from ψ_j, i.e. if ψ_j encodes a "memory" specifying ψ_i. Any process that fails this condition is logically irreversible. For example, the logical operation AND: $(p, q) \rightarrow p \wedge q$ given explicitly by:

p	q	$p \wedge q$
1	1	1
1	0	0
0	1	0
0	0	0

is logically irreversible: a unique input state (p, q) cannot be recovered whenever $p \wedge q = 0$. In general, any process that erases one or more bit values loses information about its initial state and is therefore logically irreversible. While logically reversible information processing has zero free energy cost, logically irreversible information processing has a free-energy cost of at least $\ln 2 k_B T$ per irreversibly-encoded (or erased) bit [19, 20, 21], k_B Boltzmann's constant and T temperature. Hence logically irreversible informational processes are thermodynamically irreversible at the scale at which individual bit values are encoded. Measurements of cellular energy budgets can, therefore, place strict upper limits on the bandwidths in bits of logically irreversible informational processes implemented by biomolecular processes. They thus provide a sensitive test of models that represent biomolecular processes as informational processes.

Consistent with the common assumption that quantum effects are significant only at the atomic scale and below, biomolecular processes are typically represented, e.g. in diagrams depicting metabolic or regulatory pathways, as fully classical, i.e. each molecule is represented as having a particular, determinate location, conformation, charge, etc. at every

time step. This assumption of classicality is typically carried over into molecular dynamics calculations at the Å, fs scale [22, 23]. Such processes are also typically presented as logically irreversible: any biomolecular state that can be produced from multiple precursors (i.e. any state with pathway fan-in greater than one) is, strictly speaking, encoded irreversibly, even if it spontaneously decays with high probability back to one of its multiple possible precursors. Any biomolecular process that can be represented as Markovian, in particular, is logically irreversible. Indeed a classical process on a fixed state space can only be logically reversible if some component of each state is set aside to provide a persistent memory, for the duration of the process, of the particular sequence of state transitions (i.e. the execution trace) that produced it. This is the case, for example, for reversible classical computations implemented by Toffoli gates [24]. This memory requirement can, clearly, only remain finite if each process is completed in a finite number of steps, after which the system as a whole reverts to a fixed initial state, expending the free energy required to clear its memory. Approximate state reversion may occur in spiking neurons following the refractory period, but it is not commonplace. Indeed state reversion would not, in general, be expected in systems subject to natural selection and exposed to an unpredictably-changing environment.

In contrast to classical computation, purely quantum computation implemented by a unitary operator $\mathcal{U}$ is logically reversible by definition, i.e. for each such $\mathcal{U}$, there is a unique adjoint operator $\mathcal{U}^\dagger$ such that $\mathcal{U}^\dagger\mathcal{U} = \mathbf{Id}$, the Identity operator, on all states ψ on which $\mathcal{U}$ is defined [25]. Pure unitary quantum computation, therefore, has no free energy cost. Nor does it have the memory overhead of classical reversible computation; the "memory" is effectively stored in the phase of each quantum bit (qubit), and makes itself evident through phase interference between qubit states. The free energy cost of quantum computation is, therefore, limited to the free energy cost of classically encoding the input and output states, the cost of performing classical control operations, if any, and the cost of sufficiently isolating the computational system from its environment [26]. Quantum computations implemented by quantum gates [25], for example, are classically controlled by the connection pattern of the gates, and hence incur an overhead cost that would not be borne by a single unitary operation on all inputs [27].

We show here that assuming fully-classical, logically-irreversible, biomolecular implementations of cellular information processing at the 10s of ps to ms timescales of typical macromolecular processes [22, 28] overpredicts measured cellular free energy budgets by at least 10 to 20 orders of magnitude. We conclude that cellular information processing must employ quantum coherence as a resource for reversibility in order to maintain a biologically reasonable free energy budget. We show that cellular-scale quantum coherence is not only consistent with, but supported by models of decoherence implemented at cellular or intracellular boundaries. These bioenergetic considerations complement the more purely mathematical arguments for cellular coherence previously advanced by Bordonaro and Ogryzko [29]. We suggest that consequences of cellular-scale coherence may be detectable as supra-classical behavioral correlations in pairs of daughter cells immediately following cell division.

We begin in §2 by distinguishing classical from quantum descriptions of macromolecular

states, and macroscopic, ensemble-level degrees of freedom from microscopic, implementation-level degrees of freedom. We define a cellular state space and characterizing the sector of such a space that represents conformations and localizations of proteins. We then, in §3, show that loss of quantum coherence, i.e. an irreversible quantum-to-classical transition [30, 31], imposes irreversibility of macromolecular state transitions independently of the "interpretation" of quantum theory [32, 33] employed, and even of whether standard quantum theory or a modified theory incorporating a physical "collapse" mechanism [34, 35, 36] is assumed. We move in §4 to explicit computations of protein-sector state-space dimensionality for example prokaryotes and eukaryotes, then show in §5 that the measured cellular energy budgets of these systems are 10 to 20 orders of magnitude below those required to support fully-classical state-vector propagation, and hence fully-classical information processing at the timescales of macromolecular dynamics, in the protein-sector state space. We interpret these results in §6 using a fully-general, holographic model of decoherence as the encoding of classical information by quantum interactions [37, 38, 39], and discuss predictions of this model in §7.

2 Classical versus quantum state descriptions for the protein sector

Treating any physical system as an information processing system, i.e. a computer, involves an interpretation, implicit or explicit, mapping physical degrees of freedom to informational degrees of freedom [18]. Hence a first step towards understanding cellular processes as implementing information processing is to develop an explicit model of cellular states as bearers of information. This requires distinguishing classical from quantum representations of cellular state.

2.1 Classical versus quantum state descriptions

Suppose that a system $\mathbf{S}$, which we will interpret below as a cell interacting with an external environment, has some finite set $\mathbb{F}$ of degrees of freedom, each of which can have some finite set $\mathbb{V}$ of distinct values. By assuming that $\mathbb{V}$ is finite, we are effectively limiting the values to some fixed, finite resolution that sets the scale at which states can encode information, and by assuming a fixed set $\mathbb{V}$ we are assuming, for simplicity, that each degree of freedom can have the same number of distinct values. An instantaneous *classical state* of $\mathbf{S}$ can be represented as an assignment of one value from $\mathbb{V}$ to each degree of freedom in $\mathbb{F}$, i.e. as an element of the Cartesian product $\mathbb{F} \times \mathbb{V}$. The total number of allowed states of $\mathbf{S}$ is then the cardinality $Card(\mathbb{F} \times \mathbb{V})$. Letting $Card(\mathbb{F}) = N$ degrees of freedom and $Card(\mathbb{V}) = M$ distinct values, and supposing for simplicity that $M = 2^n$, i.e. each value can be represented as a distinct n-bit string, the binary classical dimension $d_C(\mathbf{S}) = Nn$. Assuming equal *a priori* probabilities for states s of $\mathbf{S}$, both the Boltzmann entropy $S(\mathbf{S})$ and the Shannon [40] information $\mathcal{I}(s)$ in bits are given by $d_C(\mathbf{S})$.

The classical states $s \in \mathbb{F} \times \mathbb{V}$ satisfy two notable constraints:

1. **Determinate values:** No degree of freedom can be simultaneously assigned two distinct values, and

2. **Separability:** Values can be assigned to distinct degrees of freedom completely independently.

The first constraint is enforced by the definition of a state; the second is enforced by the additivity of entropies associated with distinct degrees of freedom. A system $\mathbf{S}$ exhibits quantum superposition if the first of these constraints is violated, and quantum coherence (i.e. entanglement) if the second constraint is violated. Specifically, a pure *quantum state* ψ of $\mathbf{S}$ can be represented as a normalized vector in a Hilbert space $\mathcal{H}_{\mathbf{S}}$ with $d_Q(\mathbf{S}) = NM$ and basis vectors $|s_i\rangle$ corresponding to the NM allowed classical states. We can represent such a state at time t as:

$$\psi(t) = \sum_i \alpha_i(t)|s_i\rangle \tag{1}$$

with the α_i complex coefficients satisfying the normalization condition:

$$\sum_i |\alpha_i(t)|^2 = 1 \tag{2}$$

at any t. The state $\psi(t)$ is in general not separable, i.e. there is in general no decomposition $\mathbf{S} = \mathbf{S}_1\mathbf{S}_2$ for which $\psi(t) = \psi_1(t)\psi_2(t)$. The component $\mathbf{S}_1$ cannot, in this case, be assigned a state independently of $\mathbf{S}_2$. Indeed we can assume that $\psi(t)$ is in general maximally entangled, i.e. the entanglement entropy of an arbitrarily-chosen decomposition $\mathbf{S} = \mathbf{S}_1\mathbf{S}_2$ into components of equal dimension $NM/2$ will have maximal entanglement entropy $\mathcal{S}(\mathbf{S}_1\mathbf{S}_2) \sim NM/2$. In this case, we can think of quantum coherence as "evenly distributed" across $\psi(t)$.

The dimension $d_Q(\mathbf{S}) = NM$ of quantum states of $\mathbf{S}$ is manifestly larger than the dimension $d_C(\mathbf{S}) = Nn = N\log_2 M$ of classical states of $\mathbf{S}$. Hence quantum states encode, in principle, more information that classical states. This excess information is stored as entanglement, i.e. as phase correlations between entangled components of the state. This phase correlation information serves as the "memory" that enables the perfectly reversible unitary time evolution of pure quantum states.

2.2 Individual versus ensemble-level degrees of freedom

While individual macromolecular states, e.g. the states of individual receptors or kinases, are bearers of information in processes such as signal transduction, directly measurable degrees of freedom such as cellular energy consumption per unit time are defined only at the bulk or ensemble level. The temperature T that determines the per-bit minimum energy consumption $\ln 2 k_B T$ is an ensemble-level degree of freedom. While bulk degrees of freedom

such as shape, polarity, osmolarity, or membrane voltage can clearly carry information at both subcellular and whole-cell scales, information encoded only at these macroscopic scales will be of interest here only in its role in setting boundary conditions on the encoding of molecular-scale information.

Bulk degrees of freedom are classical by definition, and the cost of encoding classical information in logically irreversible bulk state transitions, which have characteristic timescales orders of magnitude larger that macromolecular timescales, e.g. 10s of ms for neuronal postsynaptic potentials, is trivial on a per-molecule basis. A process can, moreover, be irreversible and hence energetically costly at the molecular scale, while being reversible and energetically free when described by bulk degrees of freedom such as temperature or molecular number density (i.e. concentration); individual molecular motions in an ideal gas maintained at thermal equilibrium provides an example.

Ensembles of multiple replicates of quantum systems (not of quantum *states* by the no-cloning theorem [41]) are represented as density operators $\rho_{\mathbf{S}} =_{def} \sum_j |\psi_j\rangle\langle\psi_j|$, where the states $\{\psi_j\}$ are the basis states of $\mathbf{S}$. Each replicate in such an ensemble occupies some one of the pure states ψ_j at any given time; decoherence or collapse of a quantum ensemble to a classical ensemble involves decoherence of each pure state in the ensemble. As we will in general be interested in the states of individual molecules, we will employ density operators only to represent states of ensembles of molecules, such as water, that are not of immediate interest as information bearers. In practice, density operators also provide an appropriate representation of time ensembles of pure quantum states as considered below; however, this notion of an ensemble of *quantum* states must be strictly distinguished from the idea of an ensemble of *classical* states. Thinking of a macromolecule as occupying a "random" classical state, i.e. a single classical state sampled from an ensemble of classical states, leads to erroneous bioenergetic predictions as detailed in §5 below.

2.3 Cellular state space and its protein sector

We now consider $\mathbf{S}$ to be a cell embedded in an environment $\mathbf{E}$. For states of $\mathbf{S}$ to be well-defined independently of $\mathbf{E}$, we must assume separability of $\mathbf{S}$ from $\mathbf{E}$. If both $\mathbf{S}$ and $\mathbf{E}$ are described classically, this assumption is satisfied automatically; if either $\mathbf{S}$ or $\mathbf{E}$ is described as a quantum system, a decoherence (or physical collapse) mechanism is required as discussed in §3 below.

Representing the state of an entire cell explicitly at the molecular scale would require assigning specific values to an enormously large numbers of degrees of freedom, e.g. the positions and conformations of water and other small molecules, that are not directly involved in informational processes of primary interest such as signal transduction or gene regulation. The positions and conformations of both relatively stable and relatively transient nucleic acids must also be taken into account. Here we neglect all of these, and focus exclusively on the positions and conformations of proteins. These protein degrees of freedom and their values can be considered a sector $\mathbf{P}$ of $\mathbf{S}$; we will denote its complement $\overline{\mathbf{P}}$, i.e. $\mathbf{P}\overline{\mathbf{P}} = \mathbf{S}$.

"Neglecting" $\overline{\mathbf{P}}$ corresponds, formally, to tracing (effectively, averaging) over its degrees of freedom, i.e. considering the density operator $\rho_{\mathbf{P}} = \mathrm{Tr}_{\overline{\mathbf{P}}}\rho_{\mathbf{S}}$ as a representation of the protein-sector state. As only the single system $\mathbf{P}$ is being considered, the implied ensemble is a time ensemble as discussed in §3.2 below; hence writing $\rho_{\mathbf{P}}$ automatically invokes a temporal coarse-graining. It is worth emphasizing that the information lost in this coarse-graining is lost by us as observers; *we* choose to neglect the time-dependent information encoded by $\overline{\mathbf{P}}$. Representing the state of $\mathbf{P}$ by $\rho_{\mathbf{P}}$ does not imply an information, and hence reversibility, loss by the cell, and hence does not impact the present bioenergetic considerations. As above, states of $\mathbf{P}$ and $\overline{\mathbf{P}}$ are independently well-defined only if $\mathbf{P}$ and $\overline{\mathbf{P}}$ are separable.

Cells are viable only within small, homeostatic regions of their state spaces. Maintaining their states within this homeostatic region, e.g. by preventing the denaturing of proteins into conformations incompatible with their normal functions, is one of primary energetic tasks of the cell, and is the task that is prioritized as resources become limited [42, 43]. As the fable of Schrödinger's cat [44] amply demonstrates, however, "viability" is a classical concept that assumes cell–environment separability; it is a bulk degree of freedom only. Individual states can, moreover, only be maintained within a limited region of the accessible state space for mesoscopic or larger times: the time-energy uncertainty relation $\Delta t \Delta E \geq \pi\hbar/2$ [45] allows the energy associated with individual molecules to diverge well beyond the limits of whole-cell viability as the temporal interval Δt decreases. Hence the question of classicality is intrinsically a question of scale, to which we now turn.

3 Molecular scale decoherence imposes molecular-scale irreversibility

3.1 Joint state evolution with and without decoherence

It is an axiom of standard quantum theory that time evolution of isolated systems is unitary [47]. Any loss of quantum coherence, i.e. any decoherence, is due to interactions between systems. In modifications of quantum theory that introduce a physical collapse mechanism, loss of coherence is also attributed to interaction, either with a background noise field or with gravity [48]. Hence the evolution of joint states of composite systems is critical for decoherence.

Consider a finite composite system $\mathbf{S} = \oplus_i \mathbf{S}_i$ that evolves through time, i.e. explores its composite state space. If $\mathbf{S}$ is classical, each of the $\mathbf{S}_i$ is classical and the joint state remains classical at all times. If $\mathbf{S}$ is an isolated quantum system, the axiom of unitarity applies and the joint state remains a pure quantum state at all times. If, however, we decompose $\mathbf{S}$ into two components, i.e. write $\mathbf{S} = \mathbf{S}_1\mathbf{S}_2$ and trace out the degrees of freedom of $\mathbf{S}_2$ to consider just $\rho_{\mathbf{S}_1} = \mathrm{Tr}_{\mathbf{S}_2}\rho_{\mathbf{S}}$, we can consider coherence to "dissipate" from $\mathbf{S}_1$ into $\mathbf{S}_2$ [30, 31]. This is environment-induced decoherence or, if the component into which coherence dissipates

is a background noise field or gravity, physical collapse. Efficient decoherence of $\mathbf{S}_1$ by $\mathbf{S}_2$ requires that $\mathbf{S}_2$ function as a coherence "sink" that is large enough that net coherence does not flows "backwards" into $\mathbf{S}_1$. In this case, decoherence is effectively irreversible, i.e. phase information is effectively lost by $\mathbf{S}_1$, and hence the decohered state of $\mathbf{S}_1$ is effectively classical.

Unlike dissipated heat, however, lost quantum coherence is continuously regenerated by the internal, self-interactions of both $\mathbf{S}_1$ and $\mathbf{S}_2$. Maintaining an effectively classical state of $\mathbf{S}_1$ requires recurring decoherence (or collapse) to remove coherence as it is regenerated by the self-interaction of $\mathbf{S}_1$. If the coupling between $\mathbf{S}_1$ and $\mathbf{S}_2$ and hence the decohering interaction is weak compared to the internal interactions of $\mathbf{S}_1$ and $\mathbf{S}_2$, decoherence can be considered to recur as a sequence of discrete events with characteristic time Δt_{dec} per event and period λ_{dec} between events (cf. the treatment of collapse events in [48]). In this case $\mathbf{S}_1$ and $\mathbf{S}_2$ can be treated as at least approximately separable and hence to have independently-assignable states. As pointed out in [29], achieving effective separability requires an appropriate choice of basis for the overall system $\mathbf{S}$.

In addition to erasing quantum phase information, decoherence events separated by λ_{dec} also irreversibly erase the previous *classical* state of the system being decohered, even if they then re-encode a classically indistinguishable state. Previous state erasure is irreversible due to the Born rule, i.e. to the probabilistic nature of classical-state selection,

$$P_i(t) = |\alpha_i(t)|^2 \tag{3}$$

with i the selected classical state and the $\alpha_i(t)$ as in Eq. (2). Hence the minimal energetic cost of $\ln 2k_BT$ for erasure applies at every interval λ_{dec} even if only classical state erasure is considered.

3.2 Single-molecule scale decoherence models

We consider it uncontroversial that the cell $\mathbf{S}$ and even its environment $\mathbf{E}$ can only adequately be described in quantum-theoretic terms at some suitably microscopic scale, if necessary the Planck scale, at which even spacetime must be given a quantum-theoretic description [46]. The question is, therefore, not *whether* cells are quantum systems, but rather *at what spatiotemporal scale* do they effectively cease to be quantum systems, i.e. become amenable to classical descriptions that employ bulk concepts like viability (see the discussion of this point in [10]). In line with the above, the decoherence scale must be sufficiently large in both space and time to allow effective separability. As all relevant components of cells are molecules with strong internal interactions that regenerate internal coherence, we can assume that efficient decoherence, and hence effective classicality, requires that $\lambda_{dec} \sim \Delta t_{dec}$.

The question of decoherence scale has generally been addressed not for whole cells, but for individual molecules or macromolecular constructs embedded in cellular environments that are assumed to be "effectively classical" *a priori*. Estimates of the decoherence scale

at physiological temperature, i.e. the spatiotemporal scale $(\Delta x_{dec}, \Delta t_{dec})$ at which quantum coherence is lost at $T = 310$ K, vary widely, from roughly (1 nm, 10^{-20} s) for single ions [3] due to environmental decoherence to (25 nm, 10^{-8} s) for tubulin dimers [6] due to gravitationally-induced collapse (see [31] for a general discussion of environmental decoherence estimates and [34, 49, 50, 51] for additional collapse model estimates). Proteins, nucleic acids, polysaccarides, and even smaller organic molecules are standardly represented as having determinate, separable, and therefore classical conformations and locations at the Å, fs scale in the context of molecular dynamics calculations [22, 23]. For comparison, the dynamic timescales Δt_{dyn} for typical macromolecular processes range from 10s of ps to ms [22, 28]; see Fig. 1 for a summary.

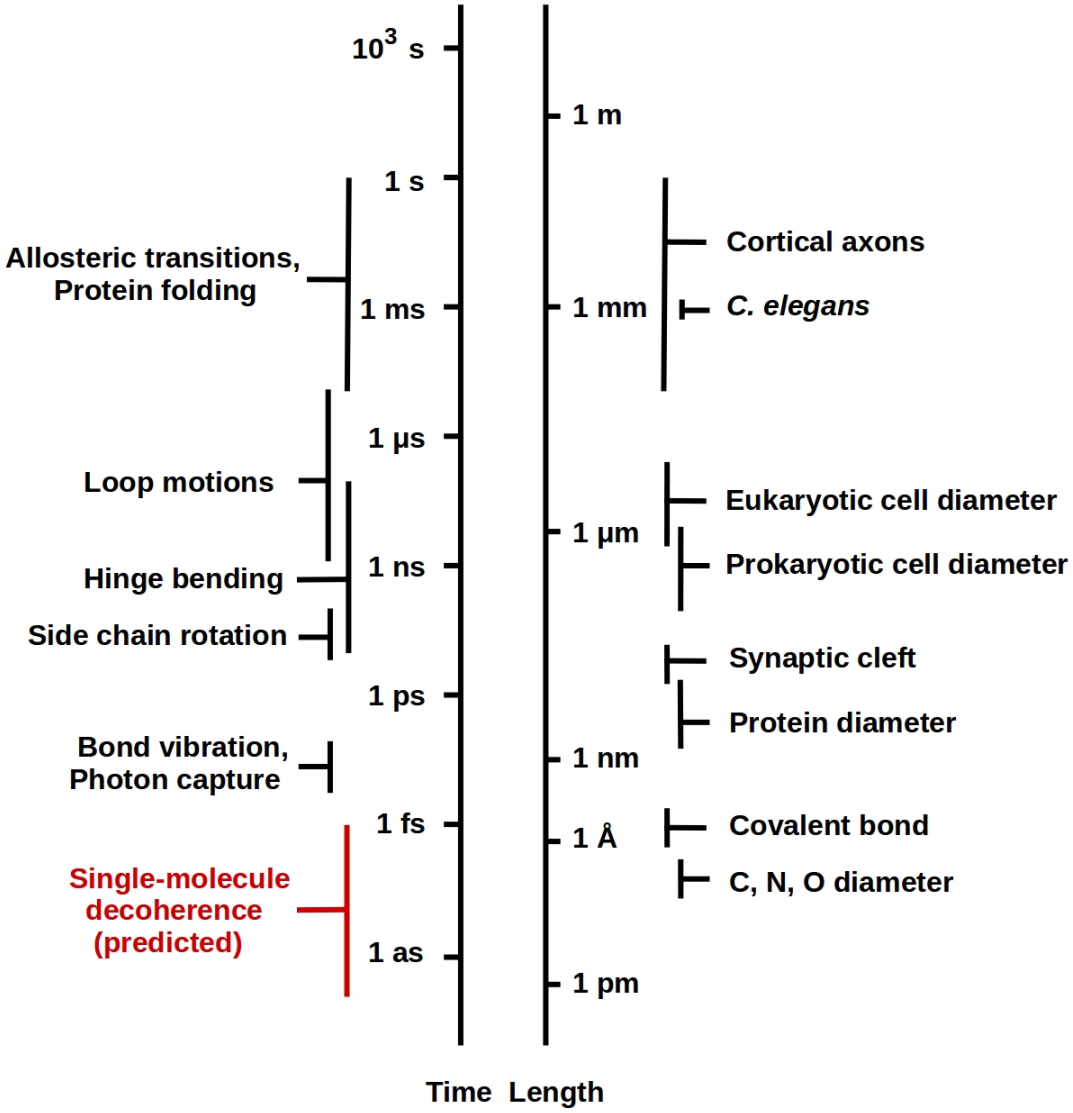

Figure 1: Temporal and spatial scales for macromolecular dynamics of interest, compared to single-molecule decoherence timescales prodicted by collisional models (Eq. (4), (5)). Further details on dynamic timescales can be found in [22]; details on cellular sizes can be found in [52].

As an explicit example, consider the model of scattering-induced decoherence given by Schlosshauer [31] following the original considerations of Joos and Zeh [53]. Here the center-of-mass position x of an object $\mathbf{X}$ of radius a is decohered at the scale Δx by multiple scattering events in which $\mathbf{X}$ is impacted by "small" environmental particles of

mass m and number density N/V. We can estimate the collisional decoherence timescale:

$$\Delta t_{dec}(\Delta x) = \Gamma^{-1}(\Delta x)^{-2} \tag{4}$$

using the long-wavelength limit for the scattering constant:

$$\Gamma = (8/3)\hbar^{-2}(N/V)(2\pi m)^{1/2}a^2(k_B T)^{3/2} \tag{5}$$

([31], Eq. 3.58 and 3.73 respectively). Taking **X** to be a typical protein with a geometric volume of roughly 50,000 Å^3 = 5·10^{-26} m^3 [54] in a water environment, $\Delta t_{dec}(\Delta x) \approx 6{\cdot}10^{-19}$ s for $\Delta x = 1$ nm, consistent with Tegmark's estimate, via an electrostatic-interaction model, of nm-scale position decoherence timescales for single ions in a cellular environment on the order of 10^{-20} s at 310 K [3]. As molecular conformation is a function of the relative positions at Angstrom scales of amino-acid side chains or other small moities, individual conformation-angle decoherence times $\Delta t_{dec}(\Delta\varphi)$ for $\Delta\varphi \approx 10^\circ$ can be expected, using this collisional model, to be roughly four orders of magnitude longer, i.e. in the fs range. In either case, we can assume the period between decoherence events $\lambda_{dec} \sim \Delta t_{dec}$ to maintain effective classicality as discussed above. For comparison, the time-energy uncertainty relation gives the minimum dissipation time scale at $\Delta E_{th} = \ln 2 k_B T$ as $\Delta t_{diss} \geq \pi\hbar/(2\Delta E_{th}) \approx 50$ fs, roughly the time scale of molecular-bond vibrational modes and considerably shorter than dynamical timescales relevant to side-chain motion or peptide-bond hinging [22].

The collisional decoherence model given by Eq. (4) and (5) assumes, as does the electrostatic model used in [3], an unstructured object **X** in an effectively thermal local environment. The decoherence-inducing interactions are, in particular, assumed to be mutually independent. It is not, however, clear that this independence assumption can be made for a typical cellular environment. The most plausible cellular candidate for a decohering environment is water undergoing thermal motion. Treating the water as an ensemble with a density operator ρ_W at the relevant scale, independence requires that any decomposition $\rho_W = \rho_{AB}$ into component ensembles A and B must be separable, i.e. $\rho_W = \rho_A\rho_B$, and have entanglement entropy of zero. These separable water ensembles must absorb coherence from macromolecular states and either dissipate it within the water state ρ_W itself or transport it to the extracellular environment, in either case while maintaining the separability of ρ_W, efficiently enough to decohere all macromolecular degrees of freedom within a timescale $\Delta t_{dec}(cell) << \Delta t_{dyn}$, the classical dynamic timescale. The existence of highly-structured hydration layers around macromolecules [55, 56], however, renders the assumption of separability for the water component of the cell unrealistic. Indeed it is far from clear that local hydration layers effectively remove coherence; they could instead function as local "memories" from which coherence information could be retrieved. There is, moreover, no obvious mechanism for "exhausting" quantum coherence from the local decohering environment of each macromolecule, whatever its structure, to the external environment of the cell, which on average is located a macroscopic distance, many orders of magnitude larger than the decoherence length, away from the site of decoherence. Similar questions can be raised

about the assumptions of dissipative (i.e. energy-conserving) collapse models, the allowed scales for which have now become highly restricted by experimental tests [57, 58].

Setting such considerations of model assumptions aside, however, any model of coherence loss at the molecular scale within cellular interiors predicts a fully-separable, effectively-classical cellular state in which each macromolecule occupies a determinate molecular-scale state (e.g. has determinate conformation and location) at every timestep of length Δt_{dec} and traverses a classical state space under the action of local forces at every timestep of length $\Delta t_{dyn} \geq \Delta t_{dec}$. Each amino-acid side chain, in particular, explores φ-angle space in discrete units of $\Delta\varphi$ in timesteps of Δt_{dec}, which we can assume to be $\approx$ fs time steps as shown in Fig. 2. Given $\Delta t_{dec}(\Delta x) << \Delta t_{dec}(\Delta\varphi)$, this variation in conformation angles is independent of the much faster (we can assume $\approx$ attosecond) exploration of whole-protein center-of-mass position space. Assuming independent peptide bonds, each individual angular evolution can be represented as a classical Markov process $\mathcal{M}_{ij} : \varphi_i \rightarrow \varphi_j$. In this picture, interactions that effectively "measure" a conformational state, e.g. binding to an enzymatic reaction center, sample a classical (ergodic) ensemble $\{\varphi_k\}$ of temporal width Δt_{int} on the order of ns to μs, i.e. $\Delta t_{int} >> \Delta t_{dec}$; averaging over this ensemble yields a coarse-grained, biologically-relevant outcome value $< \varphi >$. Classical molecular dynamics calulations at Å, fs scales model this Markovian evolution; the huge numbers of iterations needed to reach biologically-relevant time scales contribute to issues of both accuracy and feasibility [22]. Hybrid quantum mechanics/molecular mechanics (QM/MM) methods allow the treatment of small numbers of small molecules, e.g. water molecules and individual ions, as undergoing (approximately) unitary evolution within classical boundary conditions [59]. The effective Δt_{dec} in such a model is the fs-scale time step with which the boundary conditions, and hence interactions with the classical simulation are updated.

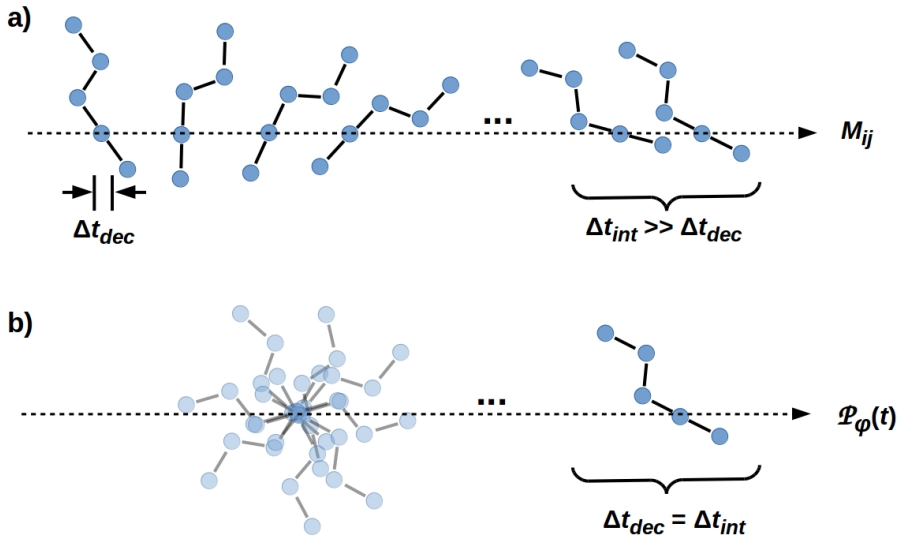

Figure 2: a) Time evolution of a conformational state (ball-and-stick cartoon) driven by a classical Markov process $\mathcal{M}_{ij}$. The conformational state is classical in every interval of length at least the decoherence time Δt_{dec}. Interactions that "measure" the conformational state, e.g. binding to an enzymatic reaction center, sample a classical ensemble $\{\varphi_k\}$ of temporal width $\Delta t_{int} >> \Delta t_{dec}$ to obtain a coarse-grained outcome $< \varphi >$. b) Time evolution of a coherent superposition $\varphi = \sum_i \alpha_i \varphi_i$ of molecular states φ_i with amplitudes α_i. Assuming separability, binding to an enzymatic reaction center with characteristic time t_{meas} effectively decoheres a particular outcome φ_k with probability $|\alpha_k|^2$.

In the opposite, quantum limit of no internal decoherence, the state of a notionally isolated degree of freedom φ evolves as a superposition $|\varphi\rangle = \sum_i \alpha_i |\varphi_i\rangle$ under the action of a unitary propagator $\mathcal{P}_{\varphi}(t)$ as discussed §2.1 above. In this case, binding to an enzymatic reaction center $\mathbf{R}$ with characteristic time Δt_{int} introduces, given an assumption of initial-state separability, external interactions that effect decoherence, i.e. $\Delta t_{dec} =_{def} \Delta t_{int}$, to some particular outcome φ_k with probability $|\alpha_k|^2$. If initial state separability is not assumed, such an interaction results in further entanglement of the joint state $|\varphi \mathbf{R}\rangle$.

Interventions into the cellular state from the external environment, e.g. to perform measurements, inevitably induce decoherence as discussed in §6 below. Hence nondisturbing measurements are essential to probe the cellular state for large-scale coherence. As measurements of total cellular energy budgets place upper limits on the total number of classical bits encoded by irreversible processes, they provide a nondisturbing, quantitative, model-independent probe for the energetic consequences of irreversible decoherence or collapse processes acting at the macromolecular scale. Such measurements involve thermal coupling and are, therefore, insensitive to the states of individual molecules. They do, however, allow quantitation of the total number of macromolecular degrees of freedom, however

distributed across individual macromolecules, that occupy determinate, separable states over macroscopic times. They therefore provide a sensitive test for bulk classicality at the macromolecular scale.

4 Empirical data fix protein sector dimensions

In order to estimate minimum energetic requirements for irreversible informational processes implemented by proteins in effectively-classical states, we first estimate the dimensionality of the protein sector **P** under a classical description. We can, without loss of generality, treat state vectors as binary-valued and estimate their dimensionality d in bits as discussed in §2.1 above. The dimensionality d(Conform) of the conformational component of **P** can then be estimated as the average number of bits required to specify a single protein conformation times the number of proteins. Assuming an average length of 333 amino acids, specifying the conformation of a typical protein *ab initio* requires roughly 10^3 bits [60]; restricting each amino-acid side chain to one of three possible configurations would decrease this to an average of 10 bits/protein. The protein content of cells can be estimated roughly as 40% of dry mass [61]; measured values in representative species are reviewed in [52]. Mean per-cell mass values for four taxonomic groups of prokaryotes [62] give estimated d(Conform) as shown in Table 1.

Table 1: Conformational state space dimension d(Conform) for four taxonomic groups of prokaryotes estimated using 10^3 bits per protein [60] and proteins/cell interpolated by cell volume from exemplars given in [52] Table 1. Localization state space dimension d(Local) estimated using a typical protein geometric volume of 50,000 Å^3 $= 5 \cdot 10^{-26}$ m^3 [54] and cell volumes estimated using 1 gm/ml from mass data given in [62] Table 1. Mean power consumption from [62] Table 1 converted to bits/s using 1 bit $\equiv_{def}$ $3 \cdot 10^{-21}$ J. Maximum computation rates f_{max} are for fully-classical computation on the total protein state space.

	Proteobacteria	Cyanobacteria	Firmicutes	Archaea
d(Conform)	$2.6 \cdot 10^9$	$4.2 \cdot 10^{10}$	$3.5 \cdot 10^8$	$3.5 \cdot 10^8$
d(Local)	$3.6 \cdot 10^7$	$5.6 \cdot 10^8$	$7.0 \cdot 10^6$	$6.0 \cdot 10^6$
d(Protein)	$9.4 \cdot 10^{16}$	$2.3 \cdot 10^{19}$	$2.4 \cdot 10^{15}$	$2.1 \cdot 10^{15}$
Power (fW)	20	84	2.8	4.2
Power (Mbits/s)	6.7	28	0.93	1.4
f_{max} (Hz)	$7.1 \cdot 10^{-11}$	$1.2 \cdot 10^{-12}$	$3.9 \cdot 10^{-10}$	$6.7 \cdot 10^{-10}$

The dimensionality d(Local) of the localization component of **P** can be estimated from per-cell volume given an average protein volume of 50,000 Å^3 [54] as employed above. These estimates effectively assume that all proteins are cytosolic; as membrane-bound or other compartmentalized proteins must be actively transported to their functional locations, this is not an unreasonable assumption from a bioenergetic perspective. Mean values

for prokaryotes are given in Table 1; d(Local) is roughly two orders of magnitude below d(Conform) across taxonomic groups.

The total dimension d(Protein) is computed assuming that conformation and localization are independent. This is again an approximation, particularly for membrane-bound proteins. As seen below, however, even decreasing values of d(Protein) by an order of magnitude to account for non-independence would have no qualitative effect.

Tables 2 and 3 summarize values for d(Conform), d(Local), and d(Protein) for a representative unicellular eukaryotes [63] and for average adult human [64] and adult human cerebellar and cortical neurons [65], respectively. Protein state space dimensions for eukaryotic cells are considerably higher than for prokaryotes, largely due to increased cell volume. Values for neurons are for total neuronal complement within anatomical compartments, and hence average over very large Purkinje and canonical cortical neurons and much smaller granular cells, astrocytes, etc.

Table 2: State space dimensions for four representative unicellular eukaryotes calculated as in Table 1, except cell volume data from [63]. Mean power consumption from [63] Table 1 converted to bits/s using 1 bit $\equiv_{def} 3 \cdot 10^{-21}$ J. Maximum classical computation rates f_{max} calculated as in Table 1.

	Ochromonas	*Euglena*	*Bresslaua*	*Amoeba*
d(Conform)	$1.5 \cdot 10^{11}$	$7.0 \cdot 10^{12}$	$3.3 \cdot 10^{13}$	10^{15}
d(Local)	$5 \cdot 10^{9}$	$1.4 \cdot 10^{11}$	$6.6 \cdot 10^{11}$	$2.0 \cdot 10^{13}$
d(Protein)	$7.5 \cdot 10^{20}$	$9.8 \cdot 10^{23}$	$2.2 \cdot 10^{25}$	$2.0 \cdot 10^{28}$
Power (pW)	22.5	210	1,650	10,000
Power (Gbits/s)	7.5	70	550	3,300
f_{max} (Hz)	10^{-11}	$7.1 \cdot 10^{-14}$	$2.5 \cdot 10^{-14}$	$1.6 \cdot 10^{-16}$

Table 3: State space dimensions for average adult human cells from [64], and adult human cerebellar and cortical neurons from [65]. Mean power consumption converted to bits/s using 1 bit $\equiv_{def} 3 \cdot 10^{-21}$ J; maximum classical computation rates f_{max} calculated as in Table 1.

	Average Human	Cerebellar	Cortical
d(Conform)	$2 \cdot 10^{12}$	$2 \cdot 10^{12}$	$2 \cdot 10^{12}$
d(Local)	$8 \cdot 10^{10}$	$8 \cdot 10^{10}$	$8 \cdot 10^{10}$
d(Protein)	$1.6 \cdot 10^{23}$	$1.6 \cdot 10^{23}$	$1.6 \cdot 10^{23}$
Power (pW)	1.5	42	750
Power (Gbits/s)	0.5	14	250
f_{max} (Hz)	$3.1 \cdot 10^{-15}$	$8.8 \cdot 10^{-14}$	$1.5 \cdot 10^{-12}$

Considering only protein conformation and localization clearly underestimates the dimensionality of the state space relevant to cellular information processing. Highly localized concentration gradients of Ca^{2+} and other ions, cofactors such as adenosine and guanine triphosphate (ATP and GTP), and other small molecules also play significant roles in regulating cellular state [66, 67, 68], as does localized bioelectric state [69]. Both the topological conformation and base-by-base inter-strand interaction states of nucleic acids are also significant, although typically on slower timescales [70, 71]. Hence using protein conformation and localization states to estimate the energetic cost of classical computation provides a lower limit only; more realistic values may be several orders of magnitude higher.

5 Cellular energy budgets cannot support molecular-scale classical computation

Classical computation requires updating a classical state, i.e. an N-bit string, on each computational clock cycle, independently of how many bits in the string change their values on each cycle. Computation at a clock frequency f incurs a minimal unit-time energetic cost (i.e. power consumption) of $Nf\ln 2 k_B T$ [19]. Computing with 32 GB at a clock speed of 2.3 GHz at $T = 310$ K, for example, has a minimal cost of ≈ 1.7 W, roughly 80% of the thermal design power of a commercial microprocessor with these specifications [72]. In the current setting, in which irreversibility and hence effective classicality is due to decoherence (via environmental interactions or collapse), the "clock cycle" is the period λ_{dec} between decoherence events. To compute cellular-scale power usage, we assume $\lambda_{dec} \sim \Delta t_{dec}$ as in §3.2 above. For simplicity, we will abuse notation slightly to define "1 bit" of energy as $\ln 2 k_B T \approx 3{\cdot}10^{-21}$ J at $T = 310$ K, with a corresponding power unit of bits/s. We emphasize that $\ln 2 k_B T$ is a minimal estimate that applies to all classical state changes regardless of their functional consequences. Biochemical "bit flips" with functional consequences at the cellular scale typically require ATP or GTP hydrolysis to guarantee irreversibility and hence expend on the order of 10 $k_B T$; see e.g. [16, 73] for discussion of molecular computations implemented by these higher-energy processes and [74] for a model of hydrolysis as an extended, entanglement-generating process.

Tables 1, 2, and 3 summarize mean per-cell power consumption measurements for representative prokaryotes [62], unicellular eukaryotes [63], and average adult human cells [64] and adult human cerebellar and cortical neurons [65], respectively. On average, eukaryotes consume three or more orders of magnitude more power per cell than prokaryotes, a difference attributable to both larger size and the availability of mitochondria specialized for respiration [75]. Neurons, particularly cortical neurons, consume considerably more energy than average human cells, consistent with the brain's use of roughly 20% of the whole-body energy budget in humans [76]. This energy consumption is split between signalling activity and state maintenance [77, 78]. Significantly, the entire energy budget of a large cortical neuron has been estimated to be consumed by action-potential generation and recovery [79].

As tables 1, 2, and 3 indicate, cellular power consumption falls far short of that required to maintain a fully-classical, i.e. fully-decoherent state at the fs scale of molecular dynamics calculations or even the μs scale of protein domain motions. Indeed the maximum classical computation rate f_{max} achievable with the given power consumption falls short of 1 Hz by roughly 10^{10} for prokaryotes and small eukaryotic cells up to roughly 10^{15} for larger eukaryotic cells. Even altogether ignoring protein localization, none of the cell types examined can support fully classical encoding of protein conformational state at 1 Hz. We conclude that neither prokaryotes nor eukaryotes have the metabolic resources to support fully-classical information processing at the molecular scale. Requiring classical computation rates in the kHz range of typical inter- and intra-cellular signaling processes restricts encoded classical states, and hence decoherence, to components spanning only 10^{-13} to 10^{-19} of the available protein state space. The remaining components of the state space cannot undergo decoherence at kHz frequencies with the available metabolic resources.

6 Cell-level decoherence implemented by classical encoding on intercompartmental boundaries

The most straightforward interpretation of tables 1, 2, and 3 is that intracellular decoherence (or "measurement") occurs not at the attosecond to fs time scales of molecular-scale fluctuations, but rather at the μs to ms time scales of intercompartmental or intercellular information exchange. Assuming for simplicity that intercompartmental or intercellular information exchange in eukaryotes is mediated by transmembrane proteins, we can estimate the required classical-information encoding densities from transmembrane protein densities. The density of tyrosine kinase receptors is roughly 550 per μm^2 on human HeLa cells and 1300 per μm^2 on CCRF-CEM cells [80]. Assuming $\approx$ 10 pS conductance per channel [81], cortical neurons have between 5 (dendrites) and 250 (axon initial segment) Na^+ channels per μm^2 [82]. Retinal rod cells can have on the order of 25,000 rhodopsin molecules per μm^2 in their layered outer-segment membranes [83]. Hence it seems reasonable to estimate on the order of 10^5 to 10^6 transmembrane proteins on the outer cell membrane of a typical human cell, with comparable densities on other eukaryotic cells. In the simplest model, each such protein encodes 1 bit per computational cycle.

Assuming spherical cells and power consumption from Tables 1, 2, and 3, the maximum numbers of bits that can be processed at 1 kH by typical prokaryotic and eukaryotic cells are shown as a function of surface area in Fig. 2. The data can be reproduced with a power law, bits(1 kH) = 100 + $A^{2.25}$, A the cell-surface area. Hence while the range for human cells (green) is consistent with the estimates above, processing power grows at a rate faster than linear in either external surface area ($\sim$ A) or volume ($\sim A^{1.5}$), i.e. faster than expected for allometric scaling, suggesting that classical information is also encoded at high densities on intercompartmental boundaries.

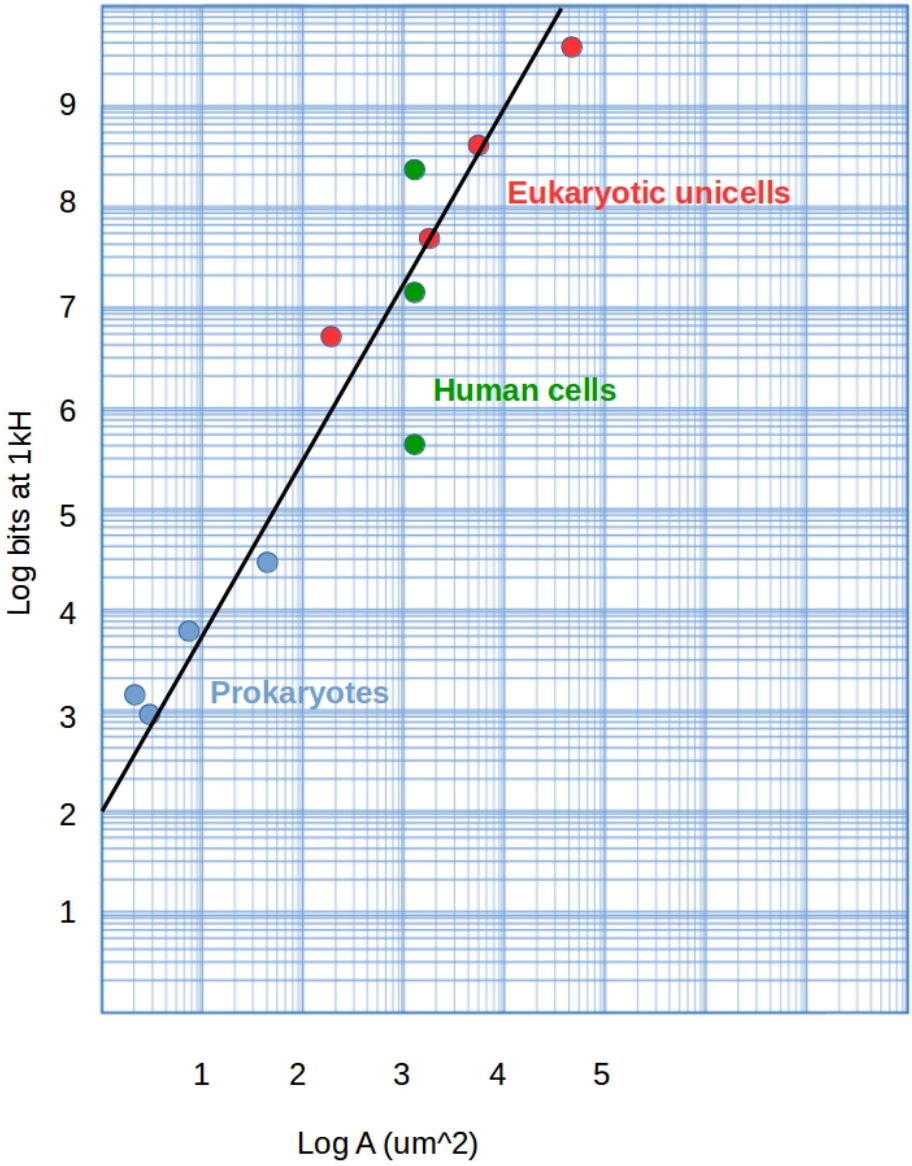

Figure 3: Maximum bits processed at 1 kH as a function of surface area, assuming spherical cells and power consumption from Tables 1, 2, and 3. Solid line is the power law: bits(1 kH) = 100 + $A^{2.25}$, A cell-surface area, assuming a spherical cell.

Decoherence and hence classical encoding only at intercompartmental or intercellular boundaries is consistent with a model of bulk cellular compartments as weakly-interacting quan-

tum systems occupying separable joint states. Here a "compartment" is simply a component that maintains an independently-definable quantum state over some time period of interest; a bounding membrane may be present but is not required. Under these conditions, the inter-compartment interactions can be viewed as einselecting [30, 84] a computational basis and holographically encoding eigenvalues in this basis on the inter-compartment boundary [37, 38, 39]. Labelling the compartments A and B and assuming standard quantum theory without physical collapse, we can write the interaction as:

$$H_{AB} = \beta^k k_B T^k \sum_i^N \alpha_i^k M_i^k, \tag{6}$$

where $k = A$ or B, the M_i^k are N Hermitian operators with eigenvalues in $\{-1, 1\}$, the $\alpha_i^k \in [0, 1]$ are such that $\sum_i^N \alpha_i^k = 1$, and $\beta^k \geq \ln 2$ is an inverse measure of k's thermodynamic efficiency that depends on the internal dynamics H_k. At each time step, A and B exchange N bits of classical information specifying the current eigenvalue of H_{AB}, entirely independently of the bulk internal dynamics H_A and H_B. These N-bit encodings constitute the only decoherent, classical information in the system. This representation of decoherence as holographic encoding is completely general, requiring none of the semi-classical assumptions of single-molecule scale models discussed in §3. The energetic cost of computation is, in this case, only the energetic cost of classical encoding N bits on the boundary; all information processing in each bulk compartment is unitary, implemented by the propagators $exp(-i/\hbar)H_k t$ and hence energetically free.

7 Prediction: Entanglement between daughter cells

A model in which decoherence is localized to intercompartmental boundaries suggests a strong and potentially testable prediction: that internal, bulk states of daughter cells may remain entangled for macroscopic times following cell division. While long-lasting mirror symmetry of cytoskeletal components and hence motion patterns as well as cell-cycle correlation of sister cells has been observed [85] and numerous examples of epigenetic inheritance [86, 87], including epigenetic inheritance of organism-scale bioeletric state [88, 89] are now known, Bell-type experiments that directly test for state entanglement in recently-separated sister cells have not, to our knowledge, yet been performed. If coherence is preserved as the above analysis suggests, perturbations of bulk biochemical state, e.g. targeting intermediate components of signal transduction pathways, in one daughter cell may be expected to affect the behavior of the other, biochemically and bioelectrically isolated, daughter cell. If observed correlations between the responses of mutually-isolated systems to perturbations of one of the systems violate Bell-type inequalities [90, 91], they cannot be explained by *a priori* classical correlation and hence provide evidence for quantum coherence. In principle, any effectively binary valued perturbations and responses can be used in such tests; in the present context, minimally-invasive probes such as ligand binding and responses such

differential gene expression may be good candidates. Such correlations may also be observable as Kochen-Specker contextuality [92, 93] or Leggett-Garg inequality [94] violations in time-series data. Recent reports of Kochen-Specker contextuality, after correction for signalling, in human decision making [95, 96] support the feasibility of detecting such effects with appropriately-designed experiments.

8 Conclusion

Consistent with single-molecule decoherence models, cellular biochemistry is standardly represented as classical at the Å, fs scale of molecular dynamics calculations. We have shown here that cellular energy budgets cannot support bulk classicality at this scale. Observed cellular energy budgets can support classical information processing at kHz rates in only 10^{-13} to 10^{-19} of the available protein state space; outside of this restricted domain, cellular information processing must be considered quantum. We suggest that biochemistry can only be treated as fully-classical at or near either the cell membrane or intercompartmental boundaries within the cell. We predict on this basis that bulk-state entanglement may be observable between recently-separated sister cells. Experimental confirmation of the availability of large-scale quantum coherence as a computational resource of cells would have immediate effects on considerations of the computational complexity and feasibility of algorithmic models of cellular information processing, e.g. of hierarchical Bayesian inference [97], as these become increasingly well developed.

While we have focused here on the measured energy budgets of extant cells, it is tempting to speculate that exceeding the limits imposed by classical thermodynamics is central, and perhaps definitional, to life as a phenomenon. Searching for quantum effects in minimal, self-organizing biochemical systems [98, 99] may shed light on this possibility.

Acknowledgements

M.L. gratefully acknowledges support by the Guy Foundation.

Conflict of Interest

The authors declare that they have no conflicts of interest relevant to the results reported here.

References

[1] Schrödinger E. 1944 *What is Life?* Cambridge, UK: Cambridge University Press.

[2] Hameroff S, Penrose R. 1996 Orchestrated reduction of quantum coherence in brain microtubules: A model for consciousness *Math. Comput. Simul.* 40: 453–480. (doi: 10.1016/0378-4754(96)80476-9)

[3] Tegmark M 2000 Importance of quantum decoherence in brain processes. *Phys. Rev. E* 61: 4194–4206. (doi: 10.1103/PhysRevE.61.4194)

[4] Hagan S, Hameroff SR, Tuszynski JA. 2002 Quantum computation in brain microtubules: Decoherence and biological feasibility. *Phys. Rev. E* 65: 061901. (doi: 10.1103/PhysRevE.65.061901).

[5] McKemmish LR, Reimers JR, McKenzie RH, Mark AE, Hush NS. 2009 Penrose-Hameroff orchestrated objective-reduction proposal for human consciousness is not biologically feasible. *Phys. Rev. E* 80: 021912 (doi: 10.1103/PhysRevE.80.021912).

[6] S. Hameroff and R. Penrose (2014) Consciousness in the universe: A review of the 'Orch OR' theory. *Phys. Life Rev.* 11: 39–78. (doi: 10.1016/j.plrev.2013.08.002)

[7] Arndt M, T. Juffmann T, Vedral V. 2009 Quantum physics meets biology. *HFSP J.* 3: 386–400. (doi: 10.2976/1.3244985)

[8] Lambert N, Chen Y-N, Cheng Y-C, Li C-M, Chen G-Y, Nori F. 2012 Quantum biology. *Nat. Phys.* 9: 10–18. (doi: 10.1038/NPHYS2474)

[9] Melkikh AV, Khrennikov A. 2015 Nontrivial quantum and quantum-like effects in biosystems: Unsolved questions and paradoxes. *Prog. Biophys. Mol. Biol.* 119: 137–161. (doi: 10.1016/j.pbiomolbio.2015.07.001)

[10] Marais A *et al.* 2018 The future of quantum biology. *J. R. Soc. Interface* 15: 20180640. (doi: 10.1098/rsif.2018.0640)

[11] Cao J *et al.* 2020 Quantum biology revisited. *Science Adv.* 6: eaaz4888 (doi: 10.1126/sciadv.aaz4888)

[12] Nijhout HF. 1990 Metaphors and the role of genes in development. *Bioessays* 12: 441–446. (doi: 10.1002/bies.950120908)

[13] Longo G, Miquel PA, Sonnenschein C, Soto AM. 2012 Is information a proper observable for biological organization? *Prog. Biophys. Mol. Biol.* 109: 108–114. (doi: 10.1016/j.pbiomolbio.2012.06.004)

[14] Turing AM 1952 The chemical basis of morphogenesis. *Phil. Trans. R. Soc. B* 237: 37–72. (doi: 10.1098/rstb.1952.0012)

[15] Polanyi M. 1968 Lifes irreducible structure. Live mechanisms and information in DNA are boundary conditions with a sequence of boundaries above them. *Science* 160: 1308–1312. (doi: 10.1126/science.160.3834.1308)

[16] Liberman EA. 1979 Analog-digital molecular cell computer. *BioSystems* 11, 111–124. (doi: 10.1016/0303-2647(79)90005-4)

[17] Rosen R. 1986 On information and complexity. In *Complexity, Language, and Life: Mathematical Approaches* (eds JL Casti, Karlqvist A), pp. 174–196. Berlin, Germany: Springer.

[18] Horsman C, Stepney S, Wagner RC, Kendon V. 2014 When does a physical system compute? *Proc. R. Soc. A* 470: 20140182. (doi: 10.1098/rspa.2014.0182)

[19] Landauer R. 1961 Irreversibility and heat generation in the computing process. *IBM J. Res. Devel.* 5: 183–195 (doi: 10.1147/rd.53.0183)

[20] C. H. Bennett CH. 1982 The thermodynamics of computation – a review. *Int. J. Theor. Phys.* 21: 905–940. (doi: 10.1007/BF02084158)

[21] Landauer R. 1999 Information is a physical entity. *Physica A* 263: 63–67. (doi: 10.1016/S0378-4371(98)00513-5)

[22] Zweir MC, Chong LT. 2010 Reaching biological timescales with all-atom molecular dynamics simulations. *Curr. Opin. Pharmacol.* 10: 745–752. (doi: 10.1016/j.coph.2010.09.008)

[23] Vlachakis D, Bencurova E, Papangelopoulos N, Kossida S. 2014 Current state-of-the-art molecular dynamics methods and applications. *Adv. Prot. Chem. Struct. Biol.* 94: 269–313. (doi: 10.1016/B978-0-12-800168-4.00007-X)

[24] Toffoli T. 1980 Reversible computing. In *Automata, Languages and Programming: Lecture Notes in Computer Science 85* (eds JW de Bakker J van Leeuwen), pp. 632–644. Berlin, Germany: Springer.

[25] Nielsen MA, Chuang IL. 2000 *Quantum Computation and Quantum Information.* New York, USA: Cambridge University Press.

[26] Deffner S, Campbell S. 2019 *Quantum Thermodynamics.* San Rafael, CA: Morgan & Claypool.

[27] Deutsch D. 2002 The structure of the multiverse. *Proc. R. Soc. London A* 458: 2911–2923. (doi: 10.1098/rspa.2002.1015)

[28] Henzler-Wildman KA, Lei M, Thai V, Kerns SJ, Karplus M, Kern D. 2007 A hierarchy of timescales in protein dynamics is linked to enzyme catalysis *Nature* 450: 913–916. (doi: 10.1038/nature06407)

[29] Bordonaro B, Ogryzko V. 2013 Quantum biology at the cellular level – Elements of the research program. *BioSystems* 112: 11–30. (doi: 10.1016/j.biosystems.2013.02.008)

[30] Zurek WH. 2003 Decoherence, einselection, and the quantum origins of the classical. *Rev. Mod. Phys.* 75: 715–775. (doi: 10.1103/RevModPhys.75.715)

[31] Schlosshauer M. 2007 *Decoherence and the Quantum Origins of the Classical* Berlin, Germany: Springer.

[32] Landsman NP. 2007 Between classical and quantum. In *Handbook of the Philosophy of Science: Philosophy of Physics* (eds J Butterfield, J Earman), pp. 417–553. Amsterdam, Netherlands: Elsevier.

[33] Cabello A. 2015 Interpretations of quantum theory: A map of madness. Preprint arXiv:1509.04711v1.

[34] Ghirardi GC.; Rimini A, Weber T. 1986 Unified dynamics for microscopic and macroscopic systems. *Phys. Rev. D* 34: 470–491. (doi: 10.1103/PhysRevD.34.470)

[35] Penrose R. 1996 On gravitys role in quantum state reduction. *Gen. Relativ. Gravit.* 28: 581–600. (doi: 10.1007/BF02105068)

[36] Weinberg S. 2012 Collapse of the state vector. *Phys. Rev. A* 85: 062116. (doi: 10.1103/PhysRevA.85.062116)

[37] Fields C, Marcianò A. 2020 Holographic screens are classical information channels. *Quant. Rep.* 2: 326. (doi: 10.3390/quantum2020022)

[38] Fields C, Glazebrook JF, Marcianò A. 2021 Reference frame induced symmetry breaking on holographic screens. *Symmetry* 13: 408 (doi: 10.3390/sym13030408)

[39] Addazi A, Chen P, Fabrocini F, Fields C, Greco E, Lulli M.; Marcianò A, Pasechnik R. 2021 Generalized holographic principle, gauge invariance and the emergence of gravity à la Wilczek. *Front. Astron. Space Sci.* 8: 563450. (doi: 10.3389/fspas.2021.563450)

[40] Shannon C. 1948 A mathematical theory of communication. *Bell Syst. Tech. J.* 27: 379–423. (doi: 10.1002/j.1538-7305.1948.tb01338.x)

[41] Wooters WK, Zurek WH. 1982 A single quantum cannot be cloned. *Nature* 299: 802–803. (doi:10.1038/299802a0)

[42] De La Fuente IM, Cortes JM, Perez-Pinilla MB, Ruiz-Rodriguez V, Veguillas J. 2011 The metabolic core and catalytic switches are fundamental elements in the self-regulation of the systemic metabolic structure of cells. *PLoS ONE* 6: e27224. (doi: 10.1371/journal.pone.0027224)

[43] Kerr R, Jabbari S, Johnston IG. 2019 Intracellular energy variability modulates cellular decision-making capacity *Nature Sci. Rep.* 9: 20196 (doi: 10.1038/s41598-019-56587-5)

[44] Schrödinger E. 1983 The present situation in quantum mechanics. In *Quantum Theory and Measurement.* (eds JA Wheeler, WH Zurek), pp. 152–167. Princeton, NJ, USA: Princeton University Press. Originally published in *Naturwissenshaften* 23, 1935.

[45] Lloyd S. 2000 Ultimate physical limits to computation. *Nature* 406: 1047–1054. (doi: 10.1038/35023282)

[46] Hawking SW. 1978 Spacetime foam. *Nucl. Phys. B* 144: 349–362. (doi:10.1016/0550-3213(78)90375-9)

[47] Von Neumann J. 1955 *Mathematical Foundations of Quantum Mechanics.* Princeton, NJ, USA: Princeton University Press. Originally published in German by Springer, 1932.

[48] Bassi A, Lochan K, Satin S, Singh TJ, Ulbricht H. 2013 Models of wave-function collapse, underlying theories, and experimental tests. *Rev. Mod. Phys.* 85: 471–527. (doi: 10.1103/RevModPhys.85.471)

[49] Adler SL. 2007 Lower and upper bounds on CSL parameters from latent image formation and IGM heating. *J. Phys. A: Math. Theor.* 40: 2935–2957. (doi: 10.1088/1751-8113/40/12/s03)

[50] Diósi L. 1989 Models for universal reduction of macroscopic quantum fluctuations. *Phys. Rev. A* 40: 1165–1174. (doi: 10.1103/PhysRevA.40.1165)

[51] Ghirardi GC, Grassi R, Rimini A. 1990 Continuous-spontaneous-reduction model involving gravity. *Phys. Rev. A* 42: 1057–1064. (doi: 10.1103/PhysRevA.42.1057)

[52] Milo R. 2013 What is the total number of protein molecules per cell volume? A call to rethink some published values. *BioEssays* 35: 1050–1055. (doi: 10.1002/bies.201300066)

[53] Joos E, Zeh HD. 1985 The emergence of classical properties through interaction with the environment. *Z. Phys. B* 59: 223–243. (doi: 10.1007/BF01725541)

[54] Chen CR, Makhatadze GI. 2015 ProteinVolume: Calculating molecular van der Waals and void volumes in proteins. *BMC Bioinform.* 16: 101. (doi: 10.1186/s12859-015-0531-2)

[55] Mattos C. 2002 Proteinwater interactions in a dynamic world. *Trends Biochem. Sci.* 27: 203–208. (doi: 10.1016/S0968-0004(02)02067-4)

[56] Levy Y, Onuchic JN. 2006 Water mediation in protein folding and molecular recognition. *Annu. Rev. Biophys. Biomol. Struct.* 35: 389–415. (doi: 10.1146/annurev.biophys.35.040405.102134)

[57] Pontin A, Bullier NP, Toroš M, Barker PF. 2020 Ultranarrow-linewidth levitated nano-oscillator for testing dissipative wave-function collapse. *Phys. Rev. Res.* 2: 023349. (doi: 10.1103/PhysRevResearch.2.023349)

[58] Vinante A, Gasbarri G, Timberlake C, Toroš M, Ulbricht H. 2020 Testing dissipative collapse models with a levitated micromagnet. *Phys. Rev. Res.* 2: 043229. (doi: 10.1103/PhysRevResearch.2.043229)

[59] Groenhof G. 2013 Introduction to QM/MM simulations. *Methods Mol. Biol.* 924: 43–66. (doi:10.1007/978-1-62703-017-5_3)

[60] Fraenkel AS. 1993 Complexity of protein folding. *Bull. Math. Biol.* 55: 1199–1210. (doi: 10.1016/S0092-8240(05)80170-3)

[61] Ho B, Baryshnikova A, Brown GW. Unification of protein abundance datasets yields a quantitative *Saccharomyces cerevisiae* proteome. *Cell Syst.* 6: 192–205. (doi: 10.1016/j.cels.2017.12.004)

[62] Makarieva AM, Gorshkov VG, Li B-L. 2005 Energetics of the smallest: do bacteria breathe at the same rate as whales? *Proc. R. Soc. B* 272: 2219–2224. (doi: 10.1098/rspb.2005.3225)

[63] Fenchel T, Finlay BJ. 1983 Respiration rates in heterotrophic, free-living protozoa. *Microbial Ecol.* 9: 99–122. (doi: 10.1007/BF02015125)

[64] Davies PCW, Rieper E, Tuszynski JA. 2013 Self-organization and entropy reduction in a living cell. *BioSystems* 111: 1–10. (doi: 10.1016/j.biosystems.2012.10.005)

[65] Herculano-Houzel S. 2011 Scaling of brain metabolism with a fixed energy budget per neuron: Implications for neuronal activity, plasticity and evolution. *PLoS ONE* 6: e17514. (doi: 10.1371/journal.pone.0017514)

[66] Clapham DE 1995 Calcium signaling. *Cell* 80: 259–268. (doi: 10.1016/0092-8674(95)90408-5)

[67] York JD 2006 Regulation of nuclear processes by inositol polyphosphates. *Biochem. Biophys. Acta* 1761: 552–559. (doi: 10.1016/j.bbalip.2006.04.014)

[68] Rosenbaum DM, Rasmussen SGF, Kobilka BK. 2009 The structure and function of G-protein-coupled receptors. *Nature* 459: 356–363. (doi: 10.1038/nature08144)

[69] Levin M. 2012 Molecular bioelectricity in developmental biology: New tools and recent discoveries. *BioEssays* 34: 205–217. (doi: 10.1002/bies.201100136)

[70] Kouzine F, Levens D, Baranello L. 2014 DNA topology and transcription. *Nucleus* 5: 195–202. (doi: 10.4161/nucl.28909)

[71] Klemm SL, Shipony Z, Greenleaf WJ. 2019 Chromatin accessibility and the regulatory epigenome. *Nat. Rev. Genet.* 20: 207–220. (doi: 10.1038/s41576-018-0089-8)

[72] Intel Corp. 2018 `https://ark.intel.com/content/www/us/en/ark/products/122590/intel-core-i3-7020u-processor-3m-cache-2-30-ghz.html`

[73] Liberman EA, Minina SV 1996 Cell molecular computers and biological information as the foundation of nature's laws. *BioSystems* 38, 173–177. (doi: 10.1016/0303-2647(95)01588-4)

[74] Matsuno K, Paton, RC. 2000 Is there a biology of quantum information? *BioSystems* 55: 39–46. (doi: 10.1016/S0303-2647(99)00081-7)

[75] Lane N, Martin W. 2010 The energetics of genome complexity. *Nature* 467: 929–934. (doi: 10.1038/nature09486)

[76] Magistretti PJ, Allaman I. 2015 A cellular perspective on brain energy metabolism and functional imaging. *Neuron* 86: 883–901. (doi: 10.1016/j.neuron.2015.03.035)

[77] Hyder F, Rothman DL, Bennett MR. 2013 Cortical energy demands of signaling and nonsignaling components in brain are conserved across mammalian species and activity levels. *Proc. Natl. Acad. Sci. USA* 110: 3549–3554. (doi: 10.1073/pnas.1214912110)

[78] Bordone MP *et al.* 2020 The energetic brain – A review from students to students. *J. Neurochem.* 151: 139–165. (doi: 10.1111/jnc.14829)

[79] Georgiev DD, Kolev SK, Cohen E, Glazebrook JF. 2020 Computational capacity of pyramidal neurons in the cerebral cortex. *Brain Res.* 1748: 147069. (doi: 10.1016/j.brainres.2020.147069)

[80] Chen Y, Munteanu AC, Huang Y-F, Phillips J, Zhu Z, Mavros M, Tan W. 2009 Mapping receptor density on live cells by using fluorescence correlation spectroscopy. *Chemistry* 15: 5327–5336. (doi: 10.1002/chem.200802305)

[81] Negulyaev YA, Khaitlina SY, Hinssen H, Shumilina EV, Vedernikova EA. 2000 Sodium channel activity in leukemia cells is directly controlled by actin polymerization. *J. Biol. Chem.* 275: 40933–40937. (doi: 10.1074/jbc.M008219200)

[82] Kole MHP, Ilschner SU, Kampa BM, Williams SR, Rubin PC, Stuart GJ. 2008 Action potential generation requires a high sodium channel density in the axon initial segment. *Nat. Neurosci.* 11: 178–186. (doi: 10.1038/nn2040)

[83] Molday RS, Moritz OL. 2015 Photoreceptors at a glance. *J. Cell Sci.* 128: 4039–4045. (doi: 10.1242/jcs.175687)

[84] Ollivier H, Poulin D, Zurek WH. 2005 Environment as a witness: Selective proliferation of information and emergence of objectivity in a quantum universe. *Phys. Rev. A* 72: 042113. (doi: 10.1103/PhysRevA.72.042113)

[85] Albrecht-Buehler G. 1977 Daughter 3T3 cells. Are they mirror images of each other? *J. Cell Biol.* 72: 595–603. (doi: 10.1083/jcb.72.3.595)

[86] Jablonka E, Lachmann M, Lamb MJ. 1992 Evidence, mechanisms and models for the inheritance of acquired characters. *J. Theor. Biol.* 158: 245–268. (doi: 10.1016/S0022-5193(05)80722-2)

[87] Cunliffe VT. 2015 Experience-sensitive epigenetic mechanisms, developmental plasticity, and the biological embedding of chronic disease risk. *WIRES Syst. Biol. Med.* 7: 53–71. (doi: 10.1002/wsbm.1291)

[88] Durant F, Morokuma J, Fields C, Williams K, Adams DS, Levin M. 2017 Long-term, stochastic editing of regenerative anatomy via targeting endogenous bio-electric gradients. *Biophys. J.* 112: 2231–2243. (doi: 10.1016/j.bpj.2017.04.011)

[89] Durant F, Bischof J, Fields C, Morokuma J, LaPalme J, Hoi A, Levin M. 2019 The role of early bioelectric signals in the regeneration of planarian anterior-posterior polarity. *Biophys. J.* 116: 948–961. (doi: 10.1016/j.bpj.2019.01.029)

[90] Bell JS. 1964 On the Einstein-Podolsky-Rosen paradox. *Physics* 1: 195–200. (doi: 10.1103/PhysicsPhysiqueFizika.1.195)

[91] Fine A. 1982 Hidden variables, joint probability, and the Bell inequalities. *Phys. Rev. Lett.* 48: 291–295. (doi: 10.1103/PhysRevLett.48.291)

[92] Kochen S, Specker EP. 1967 The problem of hidden variables in quantum mechanics. *J. Math. Mech.* 17: 59–87. `https://www.jstor.org/stable/24902153`

[93] Mermin D. 1993 Hidden variables and the two theorems of John Bell. *Rev. Mod. Phys.* 65: 803–815. (doi: 10.1103/RevModPhys.65.803)

[94] Emary C, Lambert N, Nori F. 2013 Leggett-Garg inequalities. *Rep. Prog. Phys.* 77: 016001. (doi: 10.1088/0034-4885/77/1/016001)

[95] Cervantes VH, Dzhafarov EN. 2018 Snow Queen is evil and beautiful: Experimental evidence for probabilistic contextuality in human choices. *Decision* 5: 193–204. (doi: 10.1037/dec0000095)

[96] Basieva I, Cervantes VH, Dzhafarov EN, Khrennikov A. 2019 True contextuality beats directs influences in human decision making. *J. Expt. Psychol. General* 148: 1925–1937. (doi: 10.1037/xge0000585)

[97] Friston KJ. 2013 Life as we know it. *J. R. Soc. Interface* 10: 20130475. (doi: 10.1098/rsif.2013.0475)

[98] Engelhart AE, Adamala KP, Szostak JW. 2016 A simple physical mechanism enables homeostasis in primitive cells. *Nature Chem.* 8: 448–453. (doi: 10.1038/nchem.2475)

[99] Damiano L, Stano P. 2020 On the "life-likeness" of synthetic cells. *Front. Bioeng. Biotechnol.* 8: 953. (doi: 10.3389/fbioe.2020.00953)